Environmental Health
Engineering and
Management Journal

Original Article

Environmental Health
Engineering and Management

Linking ground-satellite observations with HYSPLIT Back trajectory modeling to identify dust sources affecting Western Iran: A case study in Lorestan province

Elham Borna[1] , Maryam Kiani Sadr[2*] , Seyed Ahmad Hosseini[1]

[1]Department of Environment, Kermanshah Branch, Islamic Azad University, Kermanshah, Iran
[2]Department of Environment, College of Basic Sciences, Hamedan Branch, Islamic Azad University, Hamedan, Iran

Abstract

Background: This study combined ground and satellite observations with the results of HYSPLIT model to identify the origin, transport, and deposition of sand and dust storms (SDSs) affecting Western Iran.

Methods: Field-measured dust exposure data were obtained during 2000-2014 to analyze variability of dust concentration and dust intensity at annual, monthly, and daily scales. Remote sensing measurements in this research include the analysis of a total of eight (Level 1B Calibrated Radiances 1 km (MOD021KM)) MODIS tiles selected based on interpreting the results of ground observations to capture the major SDS events occurred between 2000 and 2014.

Results: The results, indicating a sharp rise in the number of dusty days from 2008 onwards, were used as a basis to identify the spatial coverage and intensity of SDSs over the central part of the Middle East and the study province using a number of eight MODIS images. According to the back trajectory analysis of Hybrid Single-Particle Lagrangian Integrated Trajectory Model (HYSPLIT), the MODIS-derived SDSs were found to have both national and international sources. The most prevalent and powerful source was likely to initiate from deserts of Syria and Iraq by air masses coming from the Mediterranean Sea and terminate in Western Iran where the Zagros Mountains Chain blocks easterly winds.

Conclusion: Despite the evident link between timing of regional SDSs and in situ observations, the contribution of local dust sources in the west of the province should be also investigated to provide insights into the development and spread of SDS events affecting Western Iran, especially Lorestan Province.

Keywords: MODIS, HYSPLIT, Long-range transport, Dust, Lorestan

Citation: Borna E, Kiani Sadr M, Hosseini SA. Linking ground-satellite observations with HYSPLIT Back trajectory modeling to identify dust sources affecting Western Iran: A case study in Lorestan province. Environmental Health Engineering and Management Journal 2021; 8(2): 77-86. doi: 10.34172/EHEM.2021.11.

*Correspondence to:
Maryam Kiani Sadr,
Email: kianysadr@gmail.com

Introduction

Regional sand and dust storm (SDS) events are the prime concern of many countries located within the arid belt of the world (1). SDSs are driven by high-pressure gradients which boost the ground speed of winds passing over a wide region (2) to lift large quantities of soil particles - ranging from approximately 1 μm (fine particles) to 10 μm in size - from exposed (bare) soil surfaces, thus, beginning the erosion process and forming SDS events (3,4). Dust particles resulting from wind erosion accounts for nearly 40% of aerosols present in the lowest layer of Earth's atmosphere (troposphere) (5). Annually, an estimated 1000 to 2000 teragrams (1-2 billion tons) of dust are transported into the atmosphere and exert a substantial influence on regional climate and the Earth's energy balance (6). The negative impacts of SDSs are manifold.

From a metrological point of view, dust particles perturb the regional radiative budget and climate by directly absorbing and scattering solar radiation (7). They can also suppress the formation of precipitation by decreasing the size of cloud droplets and increasing the albedo of clouds (8). A variety of health risks are also associated with dust particles ranging from death in people with heart or lung diseases to asthma and irregular heartbeat depending on the size of particles (9,10). A detailed review of the effects of SDSs on agriculture is provided by Stefanski and Sivakumar who concluded that SDSs have the potential to decrease the fertility of soil and crop yield and lead to further land degradation and desertification (11).

Deserts of North Africa and the Middle East are recognized as the major sources of SDS events in the World (12), accounting for 11 (13) to 28% (14) of the

global annual dust emissions. According to the report of the United Nations Environment Assembly (UNEA), countries in these regions suffer from about $13 billion loss of gross domestic product (GDP) due to SDSs each year (15). SDSs stemming from these regions have a complex spatial and temporal variability and can affect thousands of kilometers away (16,17). For instance, an estimated 10 million tons of dust particles can reach Britain by a single SDS event from Sahara Desert (18). SDSs from the Middle East and South-West Asia can even travel longer distances due to being made up of fine particles that stem from the Tigris-Euphrates alluvial plain (a vast area covering parts of Turkey, Syria, Iraq, Iran, and Kuwait) (12). Today, the Tigris-Euphrates alluvial plain is the most active dust source in the Middle East and South-West Asia (19), where increasing desertification due to poor land management and multi-year drought have dramatically augmented the number and intensity of dust storms from this source (15).

The first step towards counteracting the current challenge of SDSs in the Middle East is to provide insights into their static and dynamic behaviors such as determining their extent, duration, intensity, and origin as well as their impacts on the Middle Eastern countries and beyond. In the literature, the main focus of studies investigating the spatio-temporal variability of regional SDS events has been primarily directed towards the utilization of remote sensing data and atmospheric transport models. In this case, Farahat confirmed the applicability of MODIS data in capturing the extent and density of dust storms from the Arabian Peninsula and the Middle East (20). Time-series MODIS data also enabled Hamidi et al to categorize the Middle Eastern SDS events into two groups: Shamal and frontal SDSs that occur in different seasons (12). Alam et al also used the aerosol optical depth (AOD) product of MODIS to investigate the development and spread of SDS events over the Middle East. They found that high-pressure zones formed over eastern Syria and northern Iraq can transport huge quantities of dust particles eastwardly from these regions to the easternmost part of the Middle East in Pakistan over the Persian Gulf (21). Moridnejad et al identified 247 dust sources in the Tigris-Euphrates alluvial plain via analyzing MODIS time-series data from 2001 to 2012 and recognized Iraq, followed by Syria as countries having the largest number of dust sources in the Middle East (22).

In addition to the static view of SDS events provided by MODIS data, atmospheric transport models have enabled better identification (and even simulation) of dust sources using back trajectory analysis. Foremost among these models is probably the Hybrid Single-Particle Lagrangian Integrated Trajectory Model (HYSPLIT) which has attracted the special attention of research community for source identification of atmospheric components (13-23). Wang et al reported that the HYSPLIT model is an essential means for understanding the emission, transport, and deposition of dust and plays a complementary role in the analysis and interpretation of in-situ and satellite observations (24). Using this model and along with the application of MODIS data, Cao et al found that the Tigris-Euphrates alluvial plain, especially the area spanning eastern Syria, Iraq, and the Iran-Iraq border is the main source of SDS events in West Asia which, in most cases (~70%), are generated by air masses coming from the Mediterranean Sea (25). By integration of field-observations, MODIS data and HYSPLIT model, the present study was conducted to identify the source of dust storms affecting Lorestan province in western Iran during 2000 to 2014. In this study, a Landsat 8 OLI-derived land use cover map and the wind-erosion sensitivity map of the province were also used for better interpretation of the results.

Materials and Methods
Study area
The focus of this research is on Lorestan province, western Iran. The province is located in the westernmost slopes of Zagros Mountain Chain stretching from the northwest to the southeast of Iran. Lorestan is a four-season province and, according to the Köppen climate classification, has a sub-humid continental climate with very cold winters (mean annual temperature of 16.9°C) (26). There are, two bare regions (with very sparse vegetation) in the west and center of the province near the capital city of Khorramabad (Figure 1).The Zagros Mountain Chain is bordered by the Tigris-Euphrates alluvial plain to the west and central Iranian desert to the east, both of which are the potential dust sources in the region. As shown in Figure 1, there are seven stations in the province known as Dorood, Imanabad, Khorramabad, Koohdasht, Noorabad, Poldokhtar, and Azna that have been collecting consistent meteorological data. Figure 1 shows the location of Lorestan Province and the stations in Iran. It should be mentioned the province is covered by rocky oak forests and highland rangelands (Figure 2).

Data
The data used in this study are based on several sections:
- Recorded data on the occurrence of dust phenomenon in synoptic stations of Lorestan
- Meteorological Organization Horizontal field of view data (8 times a day)
- Daily images of MODIS sensor in processing level 2
- Landsat images with a spatial resolution of 15-30 (m) in a period of 16 days
- Preparation of land use map and erosion map

Measurements
In this study, field-measured dust exposure data were obtained during 2000-2014 to analyze variability in dust concentration and dust intensity at annual, monthly, and daily scales. Dust concentration refers to the amount of airborne dust (particulate matters) larger than 0.25 μm in
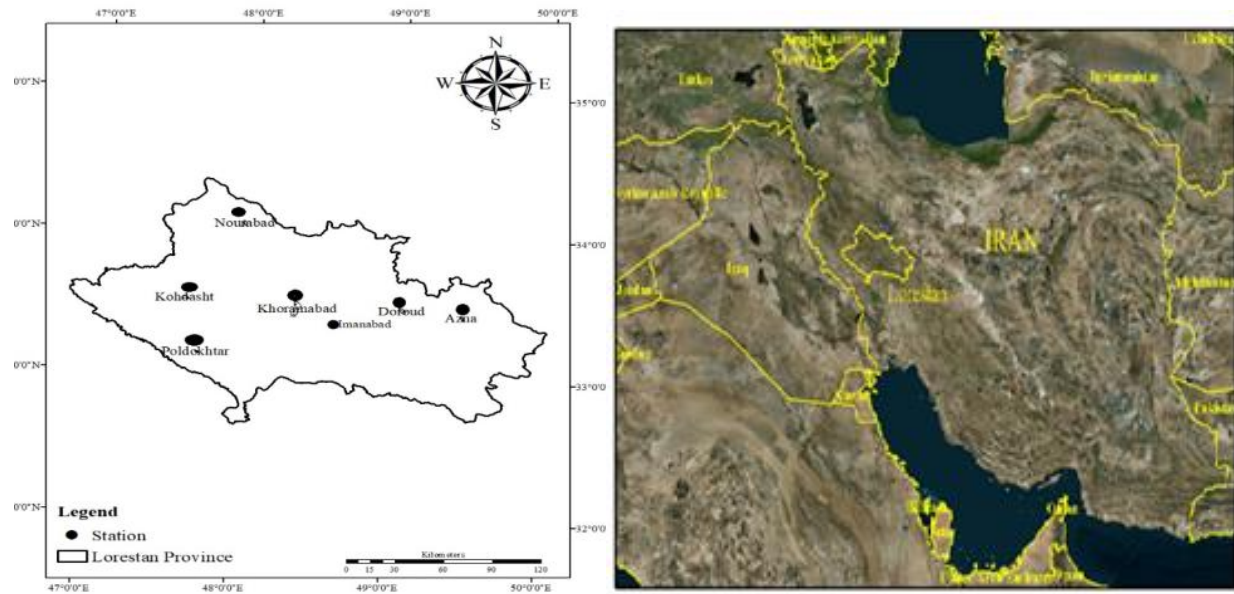
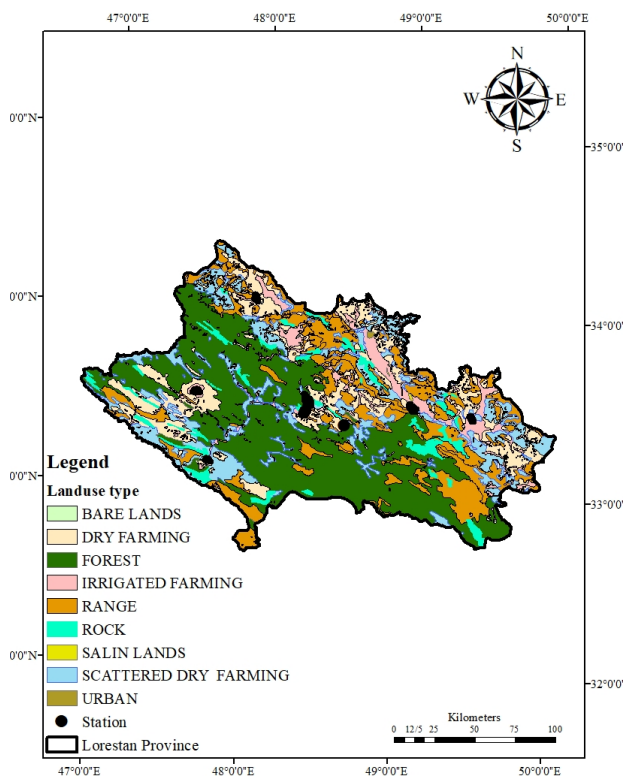**Figure 1.** Location of Lorestan province and the stations in Iran.

Figure 2. Land use cover map.

diameter while dust intensity is defined as the integrated concentration of dust particles (27). Dust intensity, as a subjective quantity, is expressed as the effect of dust on visibility impairment from a distance of 200 to 1000 m. Sand and dust at the study stations are evaluated as coarse PM_{10} to $PM_{2.5}$ concentrations to categorize each observation into dust or dust-free classes. Observations

with a high dust intensity are also reported once the visibility of sharp objects at a distance of 1000 m is significantly minimized. Through the analysis of these data, the periods during which a significant rise occurred in both concentration and intensity of SDS events were identified. The results of ground-based observations were used as a basis to perform a regional level identification of domestic and foreign dust sources using remote sensing techniques and NOAA's HYSPLIT atmospheric transport and dispersion modeling system.

Modeling using HYSPLIT
By determining the dust production centers and identifying the susceptible areas of this phenomenon, atmospheric models were used to track its propagation path. The HYSPLIT dynamic model was used to investigate the propagation paths and how this phenomenon occurred. The HYSPLIT model is a dual model for calculating the trajectory of dust movement, dispersion and simulating its sedimentation using PUFF and particle trajectories. In this model, the route and concentration of pollutants are calculated using the minimum meteorological parameters. The basis of this model is using wind speed and direction data. Thus, after processing and entering the data into the model, the propagation path for selected days along with the dust phenomenon in Lorestan province was simulated and tracked.

Systematic observation with satellite images of MODIS
Remote sensing measurements in this research include the analysis of a total of eight (Level 1B Calibrated Radiances 1 km (MOD021KM)) MODIS tiles selected based on the interpretation of the results of ground observations to capture major SDS events occurred between 2000 and

2014. MODIS provides a systematic observation of the entire Earth's surface at a revisit time of 1 to 2 days during both daytime and nighttime (28). The data collected by MODIS, aboard the Aqua and Terra systems, consist of 20 visible and short-wave infrared (SWIR) spectral channels and 16 thermal infrared wavebands, among which bands 29, 31, and 32 covering a spectral range of 8.6 to 12 μm are more suited for dust detection (29,30). In the present study, the MCTK - the MODIS Conversion Toolkit plugin for ENVI - was used to minimize the effects of atmospheric contributions and solar angle by performing the top of atmosphere reflectance calibration. The monthly AOD data were also acquired from the MOD08 Level 3 product at a resolution of 1 degree to support image processing and dust detection. The robust method of brightness temperature difference (BTD) (31) based on the wavelength channels of 29, 31, and 32 was employed to delineate the extent and magnitude of dust storm events into three classes of low, medium, and high, according to empirical thresholds.

Statistical analysis

For data analysis, the MODIS cloud mask level 2 product (MOD35) was utilized to produce a cloud mask for each MODIS tile and distinguish between cloud and dust pixels because, due to similarity in reflective characteristics, cloud areas tend to be mislabeled as dust pixels (32). It is worth mentioning that MODIS data only provide a static view of SDS events without giving information about their strength and motion. Hence, to incorporate these dimensions into the analysis, the HYSPLIT was used to identify the probable source(s) of SDSs. HYSPLIT is an atmospheric transport and dispersion model which enables tracking of emissions from a variety of sources, such as providing basic insight to the potential for long-range dust transport (33). The NCEP/NCAR global re-analysis meteorological dataset was used to calculate back air parcel trajectories for a period of 6 hours. The back trajectories were run eight times, one for each day for which SDS events were mapped using MODIS data. It was assumed that analyzing ground-based observations accompanied by regional-scale dynamic observations made by MODIS data and HYSPLIT model helps highlight the origin of SDS events occurring in the study province. A detailed Landsat 8 OLI-derived land use- cover map provided into 7 classes and a wind erosion-susceptibility map produced into 4 classes (Figure 2) was also used to discuss the role of bare lands and soil characteristics in triggering SDS events in the region.

To explain the data analysis, it can be divided into two parts. The first part deals with the extraction of dust in satellite imagery. In this paper, in order to achieve complete and comprehensive coverage of dust origin areas and the possibility of continuous monitoring, the required images of Terra satellite MODIS sensor were selected and after the formation of their mosaic, the required preprocessing and processing operations were applied using ENVI software. When a dust storm occurs, a large amount of particles accumulates together in a layered form. This thick layer of dust can absorb and reflect surface and solar radiation. Near and visible infrared channels have been used to measure the reflection of phenomena along with the MODIS Channel. The use of infrared thermal channels in measuring the luminosity temperature of phenomena is also of great importance. Comparison of the spectral properties of some phenomena, such as clouds and the earth during dust storm days, is very important in identifying and focusing on this phenomenon. Clouds are highly reflective, but their luminosity temperature is low, whereas the earth has low reflectivity, but its luminosity temperature is high. The reflection and radiant temperature of the dust storm are also between the Clouds and earth. In this paper, the luminosity and reflection temperatures of dust storms created with distinct functions are based on the extraction of the dust storm range and the estimation of its magnitude. The area that separates the dust storm from the cloud, snow, ground, etc., shows the boundary of this storm. In bands 3 and 32 of MODIS in the thermal infrared window, adsorption by other atmospheric gases is negligible and insignificant. Dust in bands 31 and 32 has very high radiance. BTD between bands 1 and 2 can be used to detect this storm. BTD can be used to identify sand from other phenomena. Therefore, other bands must also be compared and reflected from different phenomena, earth and cloud, which can be separated. The reflection of a dust storm is similar to that of the Earth as the wavelength increases. According to the spectral characteristics, the reflection of cloud and snow in the third band of MODIS reaches a maximum (0.459 ~ 0.479 μm) but in the seventh band (2.105 ~ 2.155 μm) is minimal. In fact, by knowing the reflection of waves with different wavelengths from the surface of objects, phenomena are identified. Applying spectral reflectance indicators based on the spectral reflection can estimate dust events with strong, medium, and weak intensity thresholds. By having the spectral reflection of sand, plants, soil, water, etc., it can be detected (1 μm) (increase to 2 to 4), which reflects the sand and soil, by increasing the wavelength in the bands 1 to 4 of MODIS sensor Using these spectral properties, clouds and water that have a high reflectivity in band, can be separated from sandstorms and dust. Also, to study the atmospheric conditions at the time of the storm, various meteorological parameters such as sea surface pressure, maps of the upper levels of the atmosphere, especially 1 and 2 hectopascal levels of geopotential altitude, orbital components and meridians of wind, line and tidal wave were evaluated. The data for the day of the storm, with observations four times a day with a spatial accuracy of 2.5 × 2.5 degrees arc from the Environmental Forecasting Center (NCEP) was obtained from the National Oceanic and Atmospheric Administration (NOAA).

The second part deals with tracking the path of dust

particles using the HYSPLIT model. In this research, to track the particle path using the HYSPLIT model, the backward method was used, so that at the same time, with the beginning of the first dust in the study area, the wind path was examined up to 24 hours before. In fact, the wind path was evaluated for the day before the occurrence of dust in the stations involved in this phenomenon. In the maps obtained from this model, each point on the paths ending at the station, which may be based on the output of the model and the choice of model type of square, triangle or circle, indicates the beginning of a 12-hour period and the next point of transplantation, which its end. Therefore, according to this tracking, the wind path was done for 24 hours before entering the station. Two 12-hour time intervals can be seen on each route. The asterisk on the model outputs indicates the dust stations whose length and width are given to the model. Also, the wind direction recorded by the station was shown in green, blue, and red. The height displayed at the bottom of each map from which the wind paths to the stations originate indicates the height of the path from the ground. The maps from this model show the dust transfer paths.

Results

The results of ground observations during 2000 to 2014 showed that the highest dust exposure was over the years 2008, 2009, and 2012. Except for Azna Station, a significant rise was found in the frequency of dust days (per year) from 2008 onwards, with the highest frequency of 124 days in 2009 at Dorood station (Table 1). Particularly, Imanabad station was recognized as a dust-free station from 2000 to 2005; however, the frequency of dust days at this station peaked at 79 days in 2009. In total, Dorood station had the highest frequency of dust days during the study period (675 days) while the lowest frequency of 368 days was detected at Azna station. The sharpest rise in the number of dust days was observed at Dorood station from 2007 to 2008, so that dust days grew more than 11 times from 9 to 106 days. On a monthly scale, the frequency of dust days increased consistently from 24 days in January to 736 days in July, and then, followed a consistent decreasing trend towards the last month of the year: i.e. December with the smallest number of dust days (7 days). June and July have been the dustiest months of the year. The analysis of hourly data indicated that dust concentration was relatively high from 9 to 15 o'clock, especially at 9, when the frequency of high dust concentrations was 2448 (Table 1). The concentration of dust was also found to be low during night time, especially from 18 to 3 with the lowest frequency at 0 o'clock. No dusty day was recorded over the study period at 0 o'clock at Azna, Poldokhtar, Khorramabad, Imanabad, and Dorood stations (Table 1). Similar to dust concentration, the frequency of high dust intensity started to increase from 2008. In 2009 and 2010, all stations had at least one day with a high dust intensity, with a maximum of 5 days at Poldokhtar in 2009. On a

monthly scale, the frequency of such days increased from January to July, during which a maximum of 27 days had a high dust intensity (Table 1).

According to the produced maps, the maximum area of barren lands for the western parts of the province is well visible in Figure 2. According to Figure 3, the areas with the highest sensitivity to erosion can be seen in different parts of the province. However, the western and southern parts are more sensitive than other areas. Using the results of ground observations and considering the availability of MODIS images without significant cloud coverage above the study province, a number of 8 MODIS images were selected to retrieve the magnitude and areal coverage of dust storms on 2008/07/03, 2009/07/05, 2009/07/06, 2009/07/07, 2009/07/08, 2010/06/24, 2011/04/13, and 2012/05/23. Using BTD, the quality of the images was enhanced for dust detection. In addition, the MODIS AOD products of the images were used to support accurate delineation of dust extent and magnitude. Dust extent and the qualitative magnitude classes delineated by empirical thresholds are shown in Figure 4. As shown in this figure, SDS events covered a significant part of southwestern Iran over the Iran-Iraq international border. The estimated concentration of dust and back trajectories used to determine the source and motion direction of dust are also illustrated in Figure 4. Accordingly, varying horizontal and vertical pathways of dust parcels were obtained. Broadly, however, they showed that dust storms have both domestic and foreign sources. The deserts of Iraq, Syria, and Saudi Arabia seem to be the main foreign SDS hotspots. On 2011/04/03, northern Saudi Arabia was recognized as the sole source of dust storm. On other dates, SDS events were originated from deserts of western Syria, and especially, Iraq. Among the domestic sources, Khuzestan Province in the most southwestern part of Iran was the largest and the main source of dust emissions, following by central Iranian desert (on 7- and 8-7-2009). In most cases, the concentration of dust storms was high in the southwest of the province. The highest spatial coverage and concentration of dust over the province was observed on 2009-07-09, when the western part of the province experienced a high dust concentration.

Based on the results obtained from the classification, the surface coverage of the province is in 9 main classes. Most of the vegetation, especially forest and rangeland classes, are distributed in the central parts and in the northwest southeast direction.

According to Figures 4 and 5 and examining the dust detection maps on the MODIS sensor images, it is clear that most of the recorded dust in this area is due to the formation of the nuclei of this phenomenon in the desert areas of neighboring countries, and also, incoming dust in the dust route (Khuzestan, Kermanshah, Ilam), severe dust storm has been recorded for stations in this province. Simultaneous review of wind speed and direction maps as well as implementation of tracking model for dusty days

Table 1. Frequency of dust days on annual, monthly, and daily scales

Scale		Stations							Total
		Dorood	Imanand	Kh'abad	K'dasht	N'abad	P'dokhtar	Azna	
Year	2000	46	0	35	29	22	38	11	181
	2001	2	0	4	6	2	2	2	18
	2002	9	0	20	26	9	10	11	85
	2003	25	0	45	0	28	20	73	191
	2004	6	0	14	3	11	10	5	49
	2005	14	0	29	18	14	18	8	101
	2006	1	3	26	3	6	7	2	48
	2007	9	25	58	20	24	24	4	164
	2008	106	68	88	57	71	86	39	515
	2009	124	79	106	61	71	102	57	600
	2010	100	57	100	47	53	52	35	444
	2011	64	48	66	53	44	64	33	372
	2012	69	62	88	56	39	73	41	428
	2013	77	31	54	38	28	59	33	320
	2014	23	18	26	15	5	29	14	130
Month	January	3	3	5	3	2	8	0	24
	February	28	28	46	25	13	35	13	188
	March	75	46	85	43	32	60	32	373
	April	78	48	102	57	59	71	33	448
	May	94	44	108	63	78	87	68	542
	June	130	78	139	97	87	107	73	711
	July	122	74	160	85	91	122	82	736
	August	61	37	56	34	30	54	33	305
	September	41	20	34	15	18	26	28	182
	October	36	11	20	10	15	23	5	120
	November	4	2	1	0	2	1	0	10
	December	3	0	3	0	0	0	1	7
Hour	0	0	0	0	269	111	0	0	380
	3	420	223	483	245	203	330	225	2129
	6	555	270	504	317	260	409	286	2601
	9	473	261	399	313	294	439	269	2448
	12	351	231	314	132	270	380	216	1894
	15	304	229	287	251	270	371	165	1877
	18	50	0	240	180	142	90	0	702
	21	41	0	199	146	124	87	0	597

confirms these results, because in most cases, wind speed cores are outside the study area and on dusty desert areas. Dust is formed with west-east and northwest-southeast directions, which cause the transfer of dust into Lorestan province. Considering these results and land erosion and land use maps, it can be concluded that in the study area, there are no areas that can directly and directly generate dust. However, in different parts of the province, there are areas that due to the establishment of factors such as lack of vegetation (soil and areas whose use has changed and now lack cover), there are formations with high and very high susceptibility to erosion. And the presence of gypsum and salt marls and even low humidity can aggravate the dust phenomenon if the necessary conditions are provided, such as strong winds, drought, and soil erosion. These areas are mostly located in the western and southwestern parts of the province.

Discussion

West of Iran in terms of proximity to areas is prone to dust in the West Asia region for the frequent occurrence of the phenomenon of dust over the years. SDS events are becoming more frequent and impactful in the Middle East. For instance, Iraq, which covers the majority of the

Tigris-Euphrates alluvial plain, is now experiencing about 120 dust storms and 280 dusty days in a single year, with projections indicating that this number will rise up to 300 dusty days each year in the upcoming 10 years (15). These alarming statistics are extending to a larger number of countries, dictating more national and international cooperation in combating the generation of regional SDS events (33). The majority of dust abatement efforts,

unfortunately, are in their infancy and have been most focused on accurately identifying the origin, transport, and expansion of dust storms using a combination of ground and airborne observations (13). Specifically, temporal ground and airborne observations were used in the present research to determine to which extent and degree the mountainous province of Lorestan is affected by regional and local dust storms during 2000 to 2014. According to the study of Azizi et al in the western half of Iran in the stations of Midwest and Northwest, the highest occurrence of dust was recorded in spring, while in the southern and southwestern stations of the region, the highest incidence of dust was recorded in summer, followed by autumn and winter. Also, the incidence of dust during the night hours is less than that during the day (34), which is consistent with the results of the present study (Table 1). Station-based observations suggest a sharp rise in the number of dust days from 2008 onwards. Such a trend was identified in Lorestan Province, which is strikingly consistent with the trend identified by Cao et al across the Middle East. Particularly, they found a fluctuation in the number of dust days prior to 2007 and a significant rise afterwards (25). These findings confirm that SDS events recorded in this province are parts of regional-scale ones.

To further confirm the above-mentioned claim, 8 minimally cloudy MODIS images taken near the time of high-intensity dust storms were selected to delineate the extent and the magnitude of dust storms affecting the region. In most cases, dust storms covered a vast area over the Tigris-Euphrates alluvial plain from northern Saudi
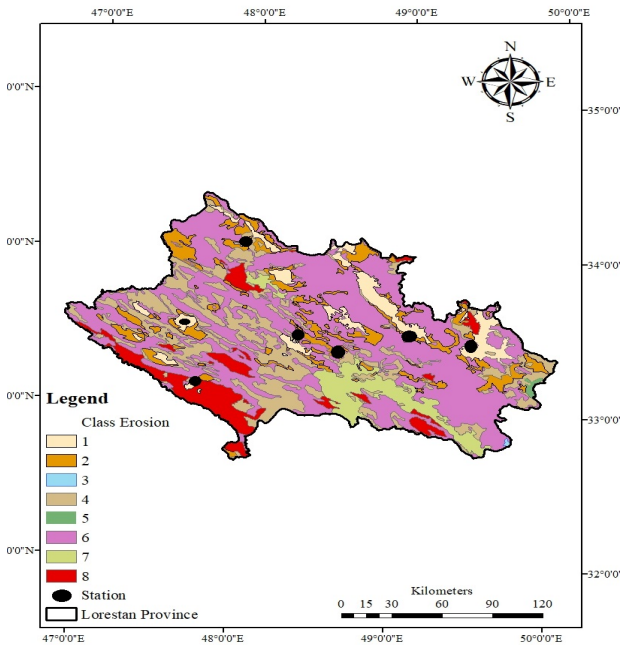

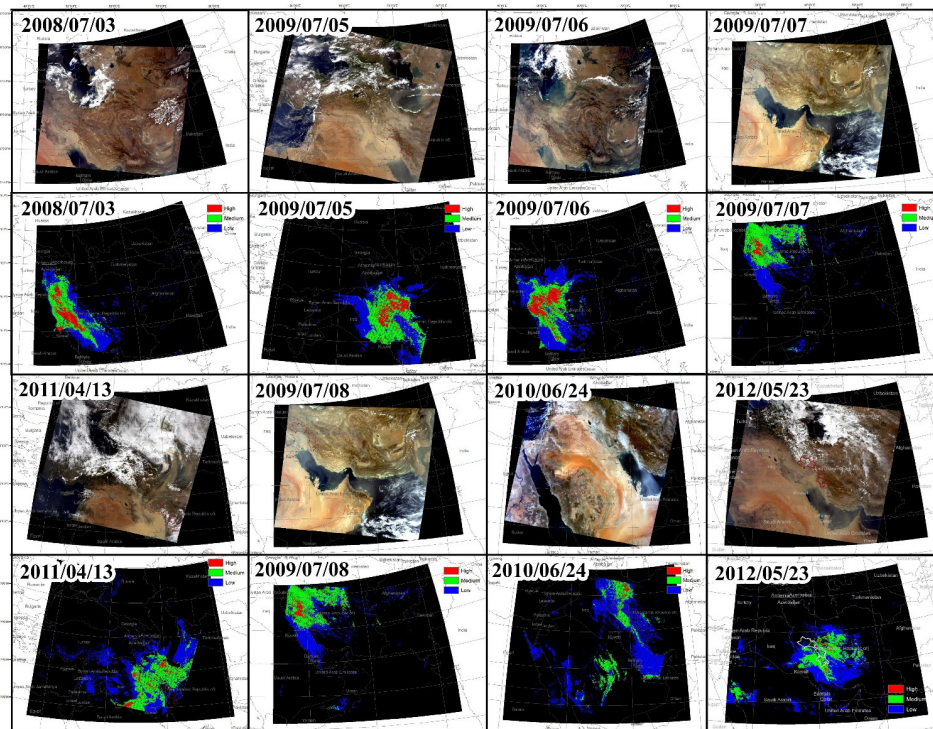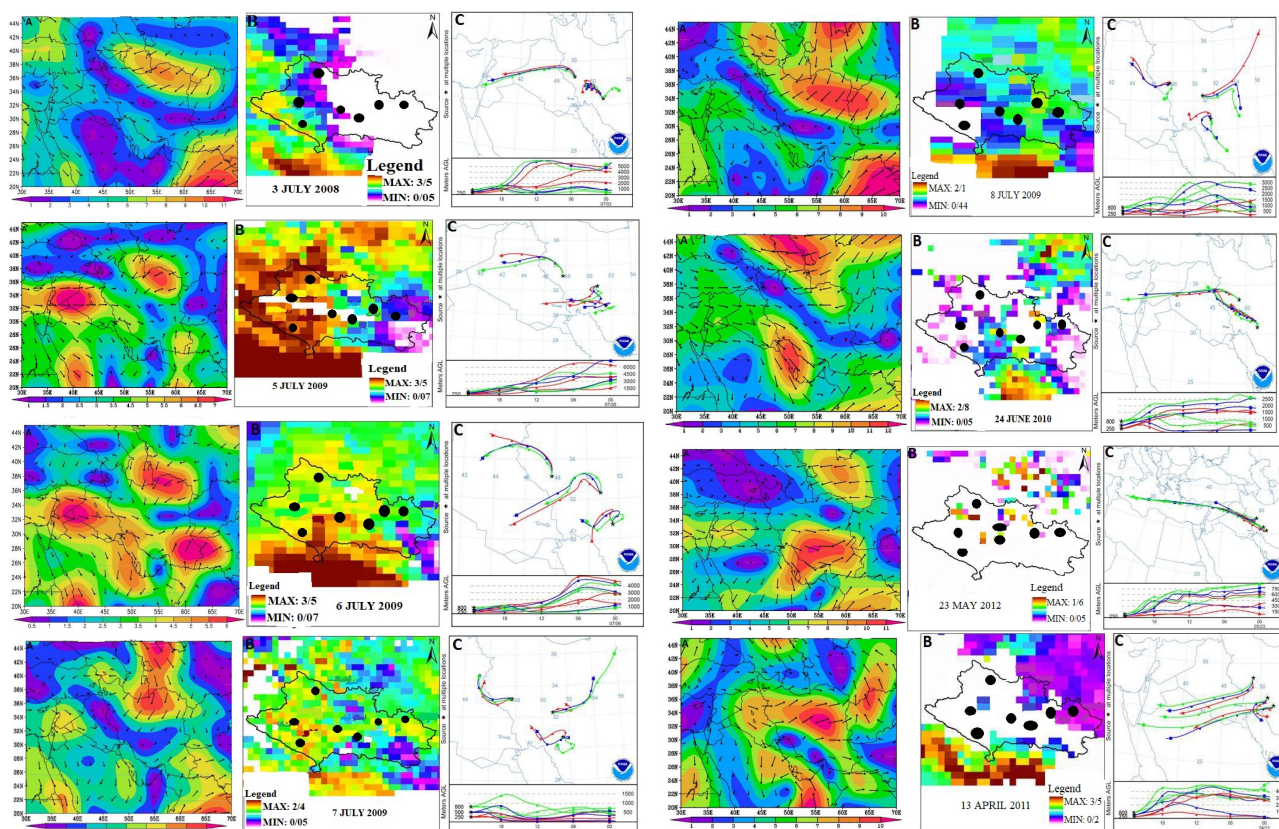Figure 3. Wind erosion-susceptibility map of Lorestan.

Figure 4. Aerial extent and intensity of SDS events delineated using MODIS data.

Figure 5. (A) Wind direction and speed (1000 hPa), (B) MODIS AOD products, (C) Results of NOAA HYSPLIT back trajectory analysis .

Arabia and the Persian Gulf to north Syria, southwest of Iran and throughout Iraq. According to the results, deserts of Iraq serve as the main sources of dust storms in the region based on the static view of dust expansion and intensity provided by processing MODIS images.

Consistent with the results of this study, Rajaee et al also reported the desert parts of northern Iraq in Tigris and Euphrates alluvial plain (a region between latitudes 33.80° N to 35.85° N and longitudes 42.00° to 44.76°E) as the main sources of dust in Ahvaz and Kermanshah (26). Also, the study of Mesbahzadeh et al showed that the Arabian deserts in Saudi Arabia and in the southwestern part of Iran can be identified as the main sources of dust in the central Iranian plateau. The other source of dust is the Hirmand Basin, located in Afghanistan and in the southeast of Iran. The results indicate that central southeast Iran could be the main dust source of internal origin and the Arabian deserts in Saudi Arabia and in southwestern Iran can be identified as the main sources of dust in the central Iranian plateau (27). These studies show that dust storms in the western and southwestern regions of Iran also affect the eastern and central regions of the country. According to a study by Jafary et al, it can be concluded that the problem of dust storms in Iran has been shifted from the west and southwest of the country to the eastern and southeastern regions (28).

The HYSPLIT model provided a dynamic view of the selected SDS events. Accordingly, the 2010-10-24 and

2012-05-23 storm pathways seem to be initiated from the Mediterranean Sea towards Cyprus and Iraq, and terminated in western Iran. A similar pathway was also identified by Cao et al. They found that this path has also an alternative destination that reaches south Iraq and Saudi Arabia, making Zagros and the study province to be less affected by this particular pathway.

Contrary to the study of Hamidi et al, in the present study, no pathway hitting western Iran from Eastern Europe was found. The 2013-04-13 SDS event started from northern Saudi Arabia and reached Iran over parts of the Persian Gulf. This pathway is likely a part of a long route identified by Alam et al (21). They found that huge quantities of dust particles (with average MODIS AOD values of >2) are carried through this pathway from Saudi Arabia and Oman over southern Iran, the Persian Gulf, and ultimately, Pakistan as the final destination. However, the most prevalent route identified in the present study extends from deserts of Syria and Iraq to western Iran. The most intense SDS event identified over Lorestan Province (2009-07-05) seems to be originated from Syria and Iraq and hit Iran through strong air masses moving from the Mediterranean Sea easterly.

Despite these pathways, some short national-wide paths were also characterized by the HYSPLIT model, which usually displayed U-turn directions, especially those covering the westernmost part of Iran (Khuzestan province). On 2009-07-07 and 2009-07-08, SDS events

hitting Lorestan Province seem to be also originated from the central Iranian desert, a pathway that has not been detected by previous studies in this field. Often in the discussion is probably the effect of Zagros Mountain Chain whose range running north-south acts as a barrier that blocks the pathways or diverts them towards the south. This effect was also evident in the results of similar studies conducted by Cao et al (25) and Hamidi et al (12). SDS events stemming from northern Saudi Arabia, as shown by Alam et al (21), move the longest distance by passing over the Persian Gulf. Despite the regional SDS events, local sources in the west of the province may also play a significant role in triggering SDS events. A large part of the province is covered by soils with a high susceptibility to wind erosion, which in combination with regional SDS events, may increase the intensity of dust storms affecting Lorestan.

Conclusion

Distribution of bare lands in the west of the Lorestan province along with easterly winds bringing massive aerosols from deserts of western Syria, northern Saudi Arabia, and Iraq, had caused western part of the province to experience frequent SDS events. Moreover, the high susceptibility of terrain to wind erosion and huge conversion of rangelands to bare and very sparse vegetation covers also highlight further attention to adopting national and international measures to combat desertification, primarily by establishing dust controlling plants. The use of ground observations helped direct identification of dust storms at the surface. Although remote sensing observations may be subject to interference from clouds, they are the only available way of providing detailed information about the intensity and spatial coverage of SDS events over vast areas. Using the combination of ground and airborne observations together with the results of HYSPLIT, it was investigated how the mountainous province of Lorestan is subject to regional SDS events. Further studies are also needed to investigate whether there is a link between ground observations and regional measurements in other provinces of Iran and also to identify all possible pathways through which easterly winds coming from the Mediterranean Sea affect west Asia.

Acknowledgments

Ethical issues

The authors hereby certify that all data collected during the research are as expressed in the manuscript, and no data from the study has been or will be published elsewhere separately.

Competing interests

The authors declare that they have no conflict of interests.

Authors' contributions

All authors have contributed in the study design, field visits, data collection and analysis, and manuscript preparation. The final version of this manuscript was reviewed and confirmed by all authors.

References

1. Krasnov H, Katra I, Friger M. Increase in dust storm related PM10 concentrations: a time series analysis of 2001-2015. J. Environ Pollut 2016; 213: 36-42. doi: 10.1016/j.envpol.2015.10.021.

2. Dementeva AL, Zhamsueva GS, Zayakhanov AS, Tsydypov VV, Ayurzhanaev AA, Azzayaa D, et al. Mass concentration of PM 10 and PM 2.5 fine-dispersed aerosol fractions in the Eastern Gobi Desert. Russian Meteorology and Hydrology 2013; 38(2): 80-7. doi: 10.3103/S1068373913020039.

3. Najafi MS, Khoshakhllagh F, Zamanzadeh SM, Shirazi MH, Samadi M, Hajikhani S. Characteristics of TSP loads during the Middle East springtime dust storm (MESDS) in Western Iran. Arabian Journal of Geosciences 2014; 7(12): 5367-81. doi: 10.1007/s12517-013-1086-z.

4. Wang G, Cheng C, Meng J, Huang Y, Li J, Ren Y. Field observation on secondary organic aerosols during Asian dust storm periods: formation mechanism of oxalic acid and related compounds on dust surface. J Atmos Environ 2015; 113: 169-76. doi: 10.1016/j.atmosenv.2015.05.013.

5. Shepherd G, Terradellas E, Baklanov A, Kang U, Sprigg WA, Nickovic S, et al. Global Assessment of Sand and Dust Storms. USA: United Nations Environment Programme; 2016.

6. Pan B, Wang Y, Hu J, Lin Y, Hsieh JS, Logan T, et al. Impacts of Saharan dust on Atlantic regional climate and implications for tropical cyclones. J Clim 2018; 31(18): 7621-44. doi: 10.1175/JCLI-D-16-0776.1.

7. Zhao C, Liu X, Leung LR, Hagos S. Radiative impact of mineral dust on monsoon precipitation variability over West Africa. J Atmos Chem Phys 2011; 11(5): 1879-93. doi: 10.5194/acp-11-1879-2011.

8. Neale RB, Richter JH, Conley AJ, Park S, Lauritzen PH, Gettelman A, et al. Description of the NCAR Community Atmosphere Model (CAM 5.0). USA: NCAR Tech Note; 2010.

9. Goudarzi G, Daryanoosh S, Godini H, Hopke PK, Sicard P, De Marco A, et al. Health risk assessment of exposure to the Middle-Eastern Dust storms in the Iranian megacity of Kermanshah. Public Health 2017; 148: 109-16. doi: 10.1016/j.puhe.2017.03.009.

10. Merrifield A, Schindeler S, Jalaludin B, Smith W. Health effects of the September 2009 dust storm in Sydney, Australia: did emergency department visits and hospital admissions increase? Environ Health 2013; 12:32. doi: 10.1186/1476-069X-12-32.

11. Stefanski R, Sivakumar MV. Impacts of sand and dust storms on agriculture and potential agricultural applications of a SDSWS. IOP Conference Series Earth and Environmental Science 2009; 7(1). doi: 10.1088/1755-1307/7/1/012016.

12. Hamidi M, Kavianpour MR, Shao Y. Synoptic analysis of

dust storms in the Middle East. Asia Pac J Atmos Sci 2013; 49(3): 279-86. doi: doi.org/10.1007/s13143-013-0027-9.

13. Tanaka TY, Chiba M. A numerical study of the contributions of dust source regions to the global dust budget. Global and Planetary Change 2006; 52(1-4): 88-104. doi: 10.1016/j.gloplacha.2006.02.002.

14. Zender CS, Bian H, Newman D. Mineral Dust Entrainment and Deposition (DEAD) model: Description and 1990s dust climatology. J Geophys Res Atmos 2003; 108(D14). doi: 10.1029/2002JD002775.

15. UNEA. UNEA-2 fact sheet: sand and dust storms.[cited 2020 Oct 12] Available from: https://uneplive.unep.org/media/docs/assessments/Sand_and_Dust_Storms_fact_sheet.pdf.

16. Yu Y, Notaro M, Liu Z, Kalashnikova O, Alkolibi F, Fadda E, et al. Assessing temporal and spatial variations in atmospheric dust over Saudi Arabia through satellite, radiometric, and station data. Journal of Geophysical Research Atmospheres 2013; 118(23): 13,253-64. doi: 10.1002/2013JD020677.

17. Zhang XX, Sharratt B, Chen X, Wang ZF, Liu LY, Guo YH, et al. Dust deposition and ambient PM 10 concentration in northwest China: spatial and temporal variability. Atmospheric Chemistry and Physics 2017; 17(3): 1699-711. doi: 10.5194/acp-17-1699-2017.

18. Wang F, Chen DS, Cheng SY, Li JB, Li MJ, Ren ZH. Identification of regional atmospheric PM10 transport pathways using HYSPLIT, MM5-CMAQ and synoptic pressure pattern analysis. Environmental Modelling & Software 2010; 25(8): 927-34. doi: 10.1016/j.envsoft.2010.02.004.

19. Al Ameri ID, Briant RM, Engels S. Drought severity and increased dust storm frequency in the Middle East: a case study from the Tigris–Euphrates alluvial plain, central Iraq. Weather 2019; 74(12): 416-26. doi: 10.1002/wea.3445.

20. Farahat A. Comparative analysis of MODIS, MISR, and AERONET climatology over the Middle East and North Africa. Ann Geophys 2019; 37: 49-64. doi: 10.5194/angeo-37-49-2019.

21. Alam K, Trautmann T, Blaschke T, Subhan F. Changes in aerosol optical properties due to dust storms in the Middle East and Southwest Asia. Remote Sens Environ 2014; 143: 216-227. doi: 10.1016/j.rse.2013.12.021.

22. Moridnejad A, Karimi N, Ariya PA. A new inventory for middle east dust source points. Environ Monit Assess 2015; 187(9):582. doi: 10.1007/s10661-015-4806-x.

23. Stein AF, Draxler RR, Rolph GD, Stunder BJ, Cohen M, Ngan F. NOAA's HYSPLIT atmospheric transport and dispersion modeling system. Bulletin of the American Meteorological Society 2015; 96(12): 2059-77. doi: 10.1175/BAMS-D-14-00110.1.

24. Wang Y, Stein AF, Draxler RR, de la Rosa JD, Zhang X. Global sand and dust storms in 2008: Observation and HYSPLIT model verification. Atmos Environ 2011; 45(35): 6368-81. doi: 10.1016/j.atmosenv.2011.08.035.

25. Cao H, Amiraslani F, Liu J, Zhou N. Identification of dust storm source areas in West Asia using multiple environmental datasets. Sci Total Environ 2015; 502: 224-35. doi: 10.1016/j.scitotenv.2014.09.025.

26. Rajaee T, Rohani N, Jabbari E, Mojaradi B. Tracing and assessment of simultaneous dust storms in the cities of Ahvaz and Kermanshah in western Iran based on the new approach. *Arabian Journal of Geosciences* 2020; 13: 461. doi: 10.1007/s12517-020-05443-2.

27. Mesbahzadeh T, Salajeghe A, Soleimani Sardoo F, Zehtabian G, Ranjbar A, Marcello MM, et al. Spatial-temporal variation characteristics of vertical dust flux simulated by WRF-chem model with GOCART and AFWA dust emission schemes (case study: central plateau of Iran). *Applied Sciences* 2020; 10(13):4536. doi: 10.3390/app10134536.

28. Jafary P, Zandkarimi A, Jannati M. Annual monitoring of dust storm in iran and adjacent areas using modis images (1396 AND 1397 HIJRI SHAMSI). Int. Arch. Photogramm. Remote Sens. Spatial Inf. Sci 2019; XLII-4(W18): 565-9. doi: 10.5194/isprs-archives-XLII-4-W18-565-2019.

29. Salehvand I, Montazeri M, Gandomkar A, Momeni M. evaluation of meteorological drought index for drought assessment and mapping in Lorestan Province in Iran. Journal of Geography, Environment and Earth Science International 2015; 2(1): 24-36. doi: 10.9734/JGEESI/2015/14375.

30. Tan M, Li X, Xin L. Intensity of dust storms in China from 1980 to 2007: a new definition. Atmos Environ 2014; 85: 215-22. doi: 10.1016/j.atmosenv.2013.12.010.

31. King MD, Menzel WP, Kaufman YJ, Tanré D, Gao BC, Platnick S, et al. Cloud and aerosol properties, precipitable water, and profiles of temperature and water vapor from MODIS. IEEE Transactions on Geoscience and Remote Sensing 2003; 41(2): 442-58. doi: 10.1109/TGRS.2002.808226.

32. Darmenov A, Sokolik IN. Identifying the regional thermal-IR radiative signature of mineral dust with MODIS. Geophysical Research Letters 2005; 32(16). L16803. doi: 10.1029/2005GL023092.

33. El-ossta E, Qahwaji R, Ipson SS. Detection of dust storms using MODIS reflective and emissive bands. IEEE Journal of Selected Topics in Applied Earth Observations and Remote Sensing 2013; 6(6): 2480-5. doi: 10.1109/JSTARS.2013.2248131.

34. Azizi M, Miri M, Nabavi SO. Detection of dust in the western half of Iran. Journal of Arid Regions Geographic Studies 2012; 2(7): 63-81. [In Persian].